Journal of Chromatography B, 870 (2008) 1–7

Contents lists available at ScienceDirect

Journal of Chromatography B

journal homepage: www.elsevier.com/locate/chromb

Features of partitioning pattern of two pancreatic enzymatic precursors: Trypsinogen and chymotrypsinogen in polyethyleneglycol–sodium citrate aqueous biphasic systems

Luciana Pellegrini Malpiedi, Guillermo Picó, Bibiana Nerli*

Chemical Physics Department, Bioseparation Laboratory, CONICET, FonCyT, Faculty of Biochemical and Pharmaceutical Sciences, National University of Rosario, S2002LRK Rosario, Argentina

ARTICLE INFO

Article history:
Received 17 November 2007
Accepted 19 March 2008
Available online 22 March 2008

Keywords:
Trypsinogen
Alpha-chymotrypsinogen
Pancreatic proteases
Aqueous two-phase systems

ABSTRACT

The partitioning behaviour of bovine trypsinogen and alpha-chymotrypsinogen, enzymatic precursors with similar physicochemical properties, was investigated in different polyethyleneglycol/sodium citrate aqueous two-phase systems. The effect of different factors such as polyethyleneglycol molecular weight, pH, tie line length and temperature was also examined. The increase of pH and the decrease of polyethyleneglycol molecular weight displaced the partitioning equilibrium of both proteins to the top phase. An enthalpy–entropy compensation pattern was observed, indicating the participation of water molecules in the partitioning mechanism. TRPz phase equilibrium showed to be more displaced to the citrate-rich phase than ChTRPz for most of the assayed systems. From a practical view, the aqueous two-phase system formed by polyethylenglycol of molecular weight 1450 and sodium citrate pH 8.20 showed the best capability for separating both proteins. When a mixture formed by equal quantities of both zymogens was partitioned in this system, significant recoveries (about 60%) were obtained. Purity values were improved significantly (84–89%) by either developing a second extractive step or increasing the top–bottom volume ratio.

1. Introduction

The development of techniques and methods for the separation and purification of proteins has been an important prerequisite for many of the advances made in the biotechnology industry. Liquid–liquid extraction using aqueous two-phase systems (ATPSs) is one of the bioseparation processes that lead to a high degree of purification and high recoveries of biological materials. This technique can be used in the early steps of a purification process (e.g., separating proteins from cell debris), replacing difficult solid–liquid separations, and also for further purification. Several advantages of ATPSs can be summarized as follows: (a) the high water content of both phases (70–80%, w/w), which means high biocompatibility and low interfacial tension, minimizing degradation of biomolecules; (b) ease of scale-up; (c) low material costs; (d) the possibility of polymer recycling [1,2].

To form the two phases, aqueous solutions of either two polymers, usually polyethyleneglycol (PEG) and dextran or a polymer (PEG) and an inorganic salt (phosphates) are required. For industrial purposes, polymer/potassium phosphate systems are the most commonly used but the high salt concentration required represents a waste disposal problem which leads to environmental concerns [3]. Previous studies have demonstrated that substitution of phosphate by citrate, a biodegradable anion, could be considered a good alternative since it has lower environmental toxicity [4].

The general properties of the aqueous two-phase systems have been studied by several researchers. However, the mechanism governing the partition of biological materials is still not well understood. The observed partition coefficient (K_p) is a result of van der Waals, hydrophobic, hydrogen bond, and ionic interactions of the biomolecules with the surrounding phase. Separation of compounds is usually attained by a systematic variation of system composition, namely the type and molecular mass of polymers, tie line (a function of the concentration of the system components), type and concentration of components or added salts, pH, temperature, etc. Development of this kind of techniques needs experimental data on partitioning of pure substances in order to know which factors affect significantly their partitioning behaviour and eventually produce a model for describing phase equilibrium [5].

Abbreviations: PEG1450, PEG3350 and PEG8000, polyethyleneglycols of average molecular masses: 1450, 3350 and 8000, respectively; TRPz, bovine trypsinogen; ChTRPz, alpha-chymotrypsinogen; ATPS, aqueous two-phase system.

* Corresponding author. Fax: +54 341 4804598.
E-mail address: bnerli@fbioyf.unr.edu.ar (B. Nerli).

1570-0232/$ – see front matter © 2008 Elsevier B.V. All rights reserved.
doi:10.1016/j.jchromb.2008.03.011

Trypsinogen (TRPz) and chymotrypsinogen (ChTRPz) are inactive enzymatic precursors which are stored in mammalian pancreas. Isolation of trypsin – the enzymatic active form of trypsinogen – from pancreatic homogenate is required since this well-known serine protease is widely used both to digest other proteins in food and leather industries and to supplement the diet of patients with pancreatic diseases [6]. Pancreatic homogenate contains several enzymatic precursors. Ribonuclease, trypsinogen and alpha-chymotrypsinogen are cationic zymogens, present in both the pancreatic juice and the zymogen granules in similar proportion. TRPz and ChTRPz, which represent about of 90% of the total cationic protein content ([TRPz]/[ChTRPz] about 1), have in common certain chemical properties. These include molecular weights (approximately 25,000 and 24,000, respectively), isoelectric points (near to 9.3) and amino acid compositions. These similarities make their complete separation difficult by means of classical methods. Besides, traditional purification methods include a first zymogen activation step followed by several affinity and ionic exchange chromatographic stages which waste long periods of time [7].

This paper reports the partitioning features of bovine trypsinogen and alpha-chymotrypsinogen in polyethyleneglycol/citrate ATPSs with the goal of selecting the ATPS which provides the optimal separation of both zymogens. Besides, driving forces involved in partitioning equilibrium of both zymogens are analyzed in order to explain their differential partitioning behaviour. This information could be used to predict a partition coefficient for the molecules of interest, TRPz and ChTRPz, which is of paramount importance in the development of a purification process from bovine pancreas using aqueous two-phase systems.

2. Materials and methods

2.1. Chemicals

Trypsinogen, alpha-chymotrypsinogen from bovine pancreas, polyethyleneglycols of average molecular masses: 1450, 3350 and 8000 (PEG1450, PEG3350, PEG8000), α-*N*-benzoyl-DL-arginine-*p*-nitroanilide (BAPNA), and 1 anilino-8-naphthalene sulfonate (ANS) were purchased from Sigma Chem. Co. and used without further purification. Citric acid, Tris–HCl, phosphoric acid and sodium chloride were of analytical quality.

2.2. Fluorescence, absorbance and circular dichroism spectra of TRPz and ChTRPz in the presence of PEGs

Absorption spectra were performed on a Jasco V-550 spectrophotometer with a slit of 2 nm and a scan rate of 200 nm min^{-1}. Fluorescence measurements were performed on an Aminco Bowman S2 spectrofluorometer using a thermostatized cuvette of 1 cm of optical pathway. The proteins were excited at 280 nm and the emission was recorded from 300 to 400 nm. Emission fluorescence spectra were corrected using the software supplied by the manufacturer. Circular dichroism (CD) spectra were performed in a Jasco J-810 spectropolarimeter, using a thermostatized cuvette of 1 mm of pathlength, the scan rate was of 50 nm min^{-1} and the bandwidth was of 1 nm. Repetitive scanning of three cycles was used. The secondary structure contents in solution were estimated from the far UV CD spectrum (190–240 nm), using a program developed by Sreerama and Woody [8] based on the Contin/ll method. Protein structure was grouped into six types: regular α-helix, distorted α-helix, regular β-strands, distorted β-strands, turns and unordered structure.

Table 1
Composition of aqueous two-phase systems formed by PEGs of different molecular weight and sodium citrate

System	Tie line number	Total Composition (% w/w)					
		pH 5.20			pH 8.20		
		PEG	Cit	TLL	PEG	Cit	TLL
PEG 1450	1	16.0	12.0	25.8	19.0	9.7	32.3
	2	15.0	12.0	22.3	17.5	9.4	29.1
	3	14.6	12.0	20.0	16.0	9.2	22.4
	4	13.9	11.7	15.0	14.4	9.0	16.1
PEG 3350	1	13.2	10.6	24.2	15.0	8.0	27.0
	2	12.3	10.5	20.5	14.0	8.0	22.5
	3	11.4	10.3	16.4	13.9	7.5	17.9
	4	10.7	10.2	11.5	11.5	7.5	12.5
PEG 8000	1	15.2	9.4	31.0	13.3	7.5	23.3
	2	14.3	9.2	28.4	12.7	7.4	18.8
	3	11.7	9.5	22.6	11.4	7.4	14.9
	4	9.6	9.5	16.5	9.7	7.3	10.0

2.3. Measurements of the protein relative surface hydrophobicity (S_o)

Although, there has been a number of attempts to establish a scale of hydrophobicity for proteins, we selected the use of ANS as a suitable fluorescent probe for non-polar sites on proteins [9], since previous reports [10] have demonstrated good correlations between the relative surface hydrophobicities determined by this method and partitioning behaviours. Aliquots (from 4 to 40 μL) of the protein solution (1.5 mM) were added to a sample containing 3 mL of ANS (final concentration 40 μM) in 50 mM sodium phosphate buffer, pH 5.50. The fluorescence emission intensity at 484 nm (when excited at 365 nm) for each protein concentration was measured on an Aminco Bowman S2 spectrofluorometer at 20 °C. The initial slope of the fluorescence intensity vs. protein concentration plot has been shown to be correlated to the protein relative surface hydrophobicity (S_o).

2.4. Preparation of the aqueous biphasic system

To prepare the biphasic aqueous systems, stock solutions of the phase components: PEG of different molecular weight 30% (w/w) and sodium citrate 25% (w/w) of a given pH were mixed according to the binodal diagram previously obtained in our laboratory [11]. The desired pH (5.20 or 8.20) of the sodium citrate solution was adjusted by the addition of sodium hydroxide. Low-speed centrifugation was used to speed up phase separation after a thorough gentle mixing of the system components, then 1 mL of each phase was mixed to reconstitute several two-phase systems in which the protein partition was assayed. The total system composition and the tie line length (TLL) are shown in Table 1.

2.5. Determination of the partition coefficient (K_p)

Partitioning behaviour of TRPz and ChTRPz was analyzed by dissolving a given amount of protein (1.5–2.1 μM total system concentration) in the two-phase systems containing 0.5 mL of each equilibrated phase. Small aliquots of the protein stock solution (1000 μM) were added to the systems (10–14 μL) in order to make the change of the total volume of each phase negligible. After mixing by inversion for 1 min and leaving it to settle for at least 120 min, the system was centrifuged at low speed for the two-phase separation. Samples were withdrawn from separated phases and after appropriate dilution (with the equilibrated phase free from protein), the protein content in each phase was determined by measuring light absorption at 280 nm. Equally diluted samples from

identical phase systems without protein were used as blanks. The partition coefficient was defined as

$$K_p = \frac{[P]_T}{[P]_B} \quad (1)$$

where $[P]_T$ and $[P]_B$ are equilibrium concentrations of the partitioned protein in the PEG and citrate-rich phases, respectively. Temperature was maintained constant and controlled to within 0.1 °C by immersing the glass tubes in a thermostatic bath. All the measurements were developed by triplicate.

2.6. Determination of thermodynamic functions associated to the protein partitioning

The TRPz and ChTRPz partition coefficients (K_p) were determined at four different temperatures (T): 281, 293, 303 and 310 K. By applying the vant Hoff equation:

$$\frac{\partial \ln K_p}{\partial(1/T)} = \frac{-\Delta H^\circ}{R} \quad (2)$$

the enthalpy change (ΔH°) associated to the protein partitioning was calculated from the slope of a $\ln K_p$ vs. $1/T$ plot. The free energy change (ΔG°) was determined from the $\Delta G^\circ = -RT \ln K_p$ and the entropy change (ΔS°) from:

$$\Delta S^\circ = \frac{\Delta H^\circ - \Delta G^\circ}{T}. \quad (3)$$

2.7. Enzyme assays

TRPz is an inactive precursor of trypsin, therefore, a previous activation step was required to determine its concentration in a mixture with ChTRPz. The TRPz activation was initiated by adding a small aliquot of trypsin ([TRPz]/[trypsin] ratio around 60) in buffer Tris–HCl 90 mM, pH 8.20 and $CaCl_2$ 45 mM [12]. The necessary time to complete the activation process was also determined by measuring the trypsin activity at different intervals until maximal value was reached.

Trypsin activity was determined with the substrate α-*N*-benzoyl-DL-arginine-*p*-nitroaniline using a method modified by Gildberg and Overbo [13]. BAPNA was used in the assay at a final concentration of 0.85 mM in 100 mM buffer Tris–HCl pH 8.20. The reaction is followed by measuring the absorbance of the released reaction product, *p*-nitroanilide, which absorbs at 400 nm (molar absorptivity of 10500 $M^{-1}\,cm^{-1}$) for 4 min. The assays were performed at constant temperature of 22 °C and the activity was calculated from the initial linear portion of the absorbance vs. time curve. The activity due to the added trypsin was subtracted in each case.

2.8. Selection of ATPS with the best separating capability

In order to select the ATPS with the best separating capability, the theoretical recovery ($R_{TRPz,B}$) and purity ($P_{TRPz,B}$) percentages of TRPz in the bottom phase that would be reached after a first extraction step, were calculated according to

$$R_{TRPz,B}(\%) = \frac{m_{TRPz,B}}{m^0_{TRPz}} 100 = \frac{1}{1 + K_{p_{TRPz}}(V_T/V_B)} 100 \quad (4)$$

where m^0_{TRPz} is the mass of trypsinogen in the initial sample and $m_{TRPz,B}$ is that corresponding to the bottom phase after reaching partitioning equilibrium, V_B and V_T are the bottom and top phase volumes. By assuming that the initial sample contains equal quantities of TRPz and ChTRPz (similar to pancreatic homogenate proportion):

$$m^0_{TRPz} = m^0_{ChTRPz} = m^0 \quad (5)$$

Table 2
Effect of PEG presence on TRPz and ChTRPz fluorescence spectrum

PEG molecular weight	Fluorescence emission			
	TRPz		ChTRPz	
	Peak position	Fluorescence intensity	Peak position	Fluorescence intensity
Buffer alone	336.0	1.451	326.0	2.510
1450	338.1	1.654	327.0	2.557
3350	338.0	1.636	328.1	2.556
8000	336.0	1.532	327.0	2.510

therefore

$$m_{TRPz,B} = m^0_{TRPz} R_{TRPz,B} = m^0 R_{TRPz,B},$$
$$m_{ChTRPz,B} = m^0_{ChTRPz} R_{ChTRPz,B} = m^0 R_{ChTRPz,B} \quad (6)$$

$$P_{TRPz,B}(\%) = \frac{m_{TRPz,B}}{m_{TRPz,B} + m_{ChTRPz,B}} 100 = \frac{R_{TRPz,B}}{R_{TRPz,B} + R_{ChTRPz,B}} 100 \quad (7)$$

$R_{TRPz,B}$ and $R_{ChRPz,B}$ were calculated from K_p values of each zymogen ($K_{p_{TRPz}}$, $K_{p_{ChRPz}}$) in the different assayed ATPSs.

2.9. Partitioning of a mixture TRPz/ChTRPz

A mixture formed by equal quantities of TRPz and ChTRPz was partitioned in the selected ATPSs. TRPz was determined in each phase according to the method previously described in order to calculate $K_{p_{TRPz}}$. Total protein content in both phases was determined by measuring the absorption at 280 nm on a Spekol 1200 spectrophotometer and $K_{p_{prot\,tot}}$ was also obtained. The recovery percentage of TRPz in the bottom phase was calculated according to Eq. (4) and TRPz purity according to

$$P_{TRPz,B}(\%) = \frac{1}{2} \frac{R_{TRPz,B}}{R_{prot\,tot,B}} 100 \quad (8)$$

where $R_{prot\,tot,B}$ is the recovery percentage of the total partitioned protein in the bottom phase. Recoveries of TRPz and total protein were checked by developing a mass balance.

3. Results and discussion

3.1. Influence of PEG presence on spectroscopic behaviour of TRPz and ChTRPz

Although ATPSs are considered to provide mild conditions for the handling of biological materials, it has been suggested that protein native conformation could be affected due to PEG–protein interactions, i.e. changes of large protein tertiary structure have been suggested [14]. It is therefore essential to evaluate the general impact that aqueous two-phase partitioning may have upon biomolecular structure.

The presence of PEGs of different MW (1450; 3350 and 8000) at 12% (w/w) did not produce any modification in TRPz and ChTRPz absorption spectra (data not shown). Besides, the native TRPz and ChTRPz fluorescence spectra (when excited at 280 nm) were analyzed in presence of PEG. Table 2 shows the height and position of emission peak of both proteins in presence and absence of PEG. Practically no shift of the emission peak but a slight change in its height was observed, which suggests the proximity of PEG molecules in the environment of the tryptophan residues on TRPz molecule. ChTRPz emission spectrum did not show to be affected by polymer presence. The effect of PEG presence for a long period of time (3 h) on the spectra was also studied. No appreciable modification either on the absorption or in the fluorescence emission was observed.

Table 3
Effect of PEG presence on TRPz and ChTRPz secondary structure

PEG molecular weight	α-Helix (%)		β-Strand (%)		Turn (%)	Unordered (%)
	r	d	r	d		
TRPz						
Buffer alone	2.50	5.00	23.40	12.50	21.10	35.50
1450	3.00	5.20	21.80	12.10	21.60	36.30
3350	1.90	4.50	23.90	12.80	21.70	35.20
8000	2.60	3.70	22.00	12.30	21.00	38.40
ChTRPz						
Buffer alone	0.60	6.70	19.90	11.90	25.80	35.10
1450	0.50	8.90	16.50	11.70	27.00	35.40
3350	0.60	6.00	20.10	12.10	24.70	36.50
8000	0.60	6.30	21.40	12.00	25.10	34.60

r, regular; d, distorted.

Circular dichroism spectra of proteins are known to be sensitive to protein structure [15]. Table 3 shows the effect of PEG at a concentration of 10% (w/w) on secondary contents of TRPz and ChTRPz in solution. No significant changes were observed, thus indicating that presence of PEG practically does not affect the secondary structure topology. No effect was observed in the near UV region (270–300 nm) of the TRPz and ChTRPz CD spectra (data not shown), which suggests that PEG does not induce micro-arrangements at the tryptophan residues accessible to solvent. These findings agree with the negligible effect of PEG presence on the fluorescence emission spectrum.

3.2. Effect of polymer molecular weight, pH and tie line length

Several factors such as PEG molecular weight, medium pH and phase composition – different tie lines – were modified in order to characterize the partitioning pattern of both zymogens. The total two-phase system compositions were selected according to the binodal diagrams obtained in our laboratory (Table 1).

Fig. 1 shows the effect of the molecular weight of PEGs on the partition of TRPz and ChTRPz. Both TRPz ($K_{p_{TRPz}}$) and ChTRPz ($K_{p_{ChTRPz}}$) partition coefficients followed the same trend, decreasing with the increase in the PEG molecular weight which has also been observed for other proteins [16]. This could be attributed to a reduction of the space available for proteins when the polymer chain length increased. The highest changes in the K_p values were observed when the PEG molecular weight varied from 1450 to 3350. Johansson at al. [17] derived an equation based on the Flory Huggins

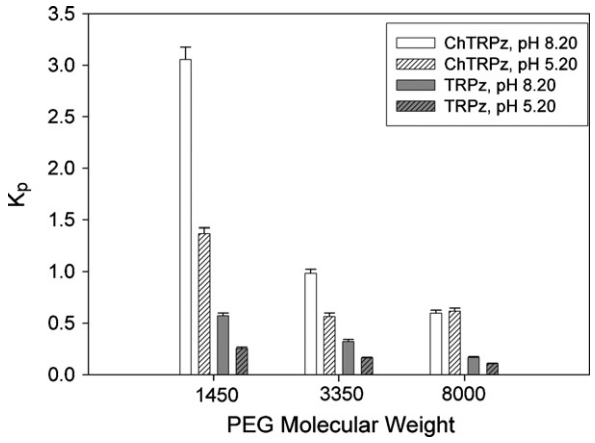

Fig. 1. Effect of PEG molecular weight and pH on the K_p value for TRPz and ChTRPz. Temperature 293 K. ATPS compositions are those corresponding to the tie line number 2. Each K_p is the average of three independent measurements. The mean estimated error for the partition coefficients was indicated.

theory that states the entropic contribution in protein partitioning

$$\ln K_p = \frac{M_{prot}}{\rho}\left(\frac{n^t}{V^t} - \frac{n^b}{V^b}\right) \quad (9)$$

M_{prot} is the molecular weight of the partitioned protein, ρ is the number of lattice sites per unit volume, V^t and V^b are the volumes of the top and bottom phases, n^t and n^b are the total number of molecules in the top and bottom phase. The n/V ratio is known as the number density of each phase. In PEG/salt systems PEG is effectively localized in the top phase. Consequently, the number of PEG molecules in the bottom phase practically do not contribute to the total number density value of this phase. Moreover, the n^b/V^b will adopt considerably higher value than the top since both water and salt which are the main bottom components, have low molecular weight. When increasing PEG molecular weight, the bottom density number remains high and practically constant while the top number density decreases, the decrease being dependent on the reciprocal of PEG molecular weight. According to this, larger changes in partitioning are expected when the molecular weight of PEG is low.

Fig. 1 also shows that the increase in pH from 5.20 to 8.20 produced an increase of the K_p value for both zymogens. According to the Albertsson equation, the K_p value depends on an electrostatic and a non-electrostatic term [2]:

$$\ln K_p = \ln K_p^0 - \frac{Z_p F \Delta\Psi}{RT} \quad (10)$$

where Z_p is the net protein charge, $\Delta\Psi$ is the interfacial potential ($\Psi_{top} - \Psi_{bottom}$) and K_p^0 is the partition coefficient of protein when electrical components ($\Delta\Psi, Z_p$) are zero. The pH could affect the partition, either by changing the charge of the solute (Z_p) or by altering the ratio of the charged species present ($\Delta\Psi$). At pH 5.20 and 8.20 both TRPz and ChTRPz are positively charged ($Z_p > 0$) because their p*I*s are 9.30 and 9.50, respectively, and $\Delta\Psi$ adopts positive values since citrate anion has shown to be excluded from PEG surface, being partitioned to the bottom phase [18]. Increasing pH from 5.20 to 8.20 will cause a Z_p decrease, while the $\Delta\Psi$ magnitude is expected to increase due to the increase in the tie line length (see Table 1) which implies an increase in the difference between the top and bottom citrate concentrations [11]. As a consequence, the K_p increase observed for both zymogens at pH 8.20 may be attributed to a prevalent effect of protein charge.

The effect of phase component concentration on the K_p was evaluated by assaying systems corresponding to different tie lines. At increasing tie line lengths, the difference between the PEG at the top and bottom phases (Δ[PEG]) also increases; therefore, $\ln K_p$ vs. Δ[PEG] plots represent a useful tool to evaluate the tie line length effect. A linear relationship (data not shown) between $\ln K_p$ and Δ[PEG] for both proteins in all the assayed systems was observed. Their slopes ($\partial \ln K_p / \partial \Delta$[PEG]) are shown in Fig. 2 and according to Diamond and Hsu [19] these values can be considered to be a function of the resultant interaction parameters between phase components such as protein–water, polymer–water and protein–polymer interactions. We observed that $\partial \ln K_p / \partial \Delta$[PEG] values for TRPz are higher than those for ChTRPz in the three assayed PEGs, which is in agreement with its higher relative surface hydrophobicity, S_o ($6.44 \times 10^{-3}\ \mu M^{-1}$ and $3.56 \times 10^{-3}\ \mu M^{-1}$ for TRPz and ChTRPz, respectively). Our results agree with those from Farruggia et al. [20] who demonstrated that the extension of the protein–PEG affinity was related to the hydrophobic superficial area of the protein exposed to the solvent.

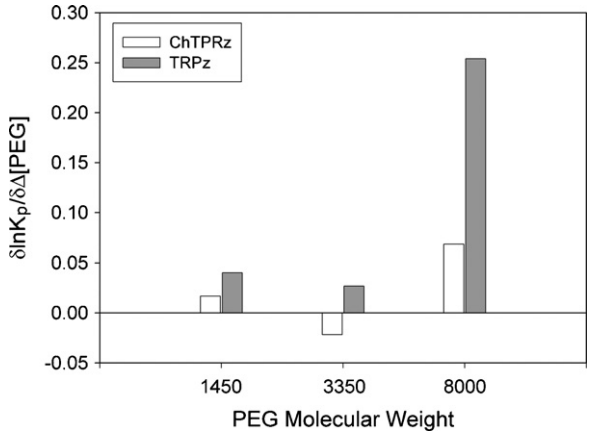

Fig. 2. Effect of PEG concentration on partitioning behaviour of TRPz and ChTRPz in PEG/citrate ATPSs of different molecular weights. Temperature 293 K. ATPS compositions are those from Table 1.

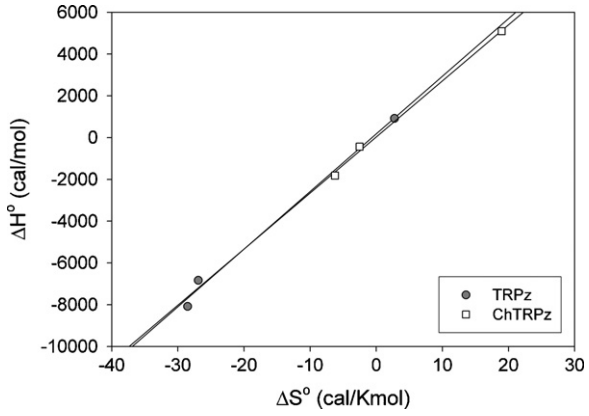

Fig. 4. Enthalpy–entropy compensation plot associated to the partitioning of TRPz and ChTRPz in PEG–citrate ATPSs, pH 8.20. Temperature 293 K. ATPS compositions: PEG1450/citrate pH 8.20 TLL 22.4% (w/w); PEG3350/citrate pH 8.20 TLL 22.5% (w/w); PEG8000/citrate pH 8.20 TLL 23.3% (w/w).

3.3. Effect of temperature: thermodynamics of the TRPz and ChTRPz partitioning

Ln K_p vs. $1/T$ plots showed linear behaviour (data not shown) for temperatures within the 293–310 K interval, thus indicating that ΔH° kept constant in this temperature range. Fig. 3 shows the ΔH° and ΔS° associated with the TRPz and ChTRPz partitioning in systems containing PEGs of different molecular weight at pH 5.20. Similar behaviour was observed at pH 8.20 (data not shown). ATPSs with similar TLLs (see figure legend) were selected in order to compare the thermodynamical behaviour. The transfer of both proteins from citrate to PEG-rich phase is either enthalpically or entropically driven depending on the PEG molecular weight. Both proteins follow a similar pattern, the enthalpy and entropy changes decrease and show a sign inversion (from positive to negative) when the MW of PEG is increased. Moreover, a ΔH° vs. ΔS° plot shows a linear relationship between them (Fig. 4), which indicates that both variables change in parallel and compensate each other to produce minor changes in the free energy of the process. This behaviour, observed in a variety of processes, is considered to be as an evidence of the participation of water molecules in the process mechanism [21]. This observation is in accordance with the Zaslavsky approach [1], which states that the effects of all factors on phase partition can be understood as a consequence of their influence on the water structure.

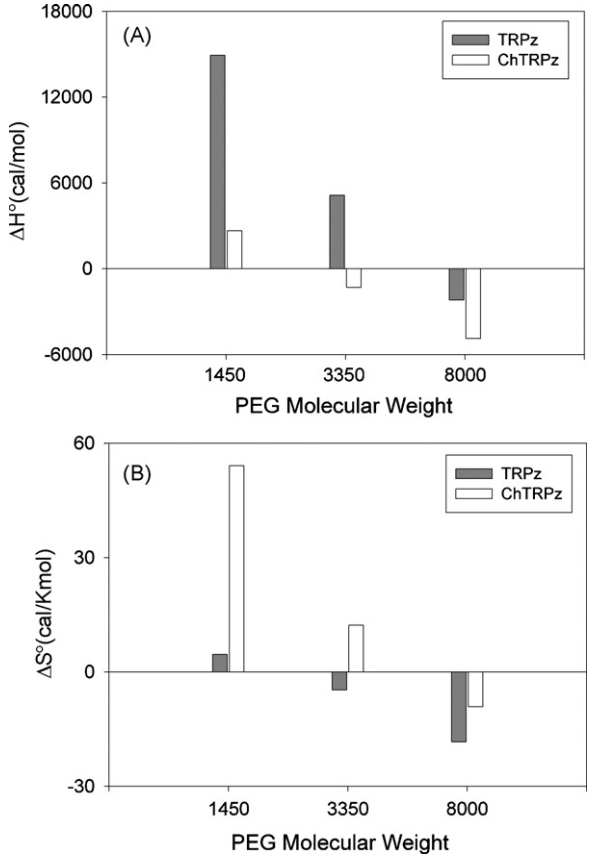

Fig. 3. Enthalpic (A) and entropic (B) changes associated to the transfer of TRPz and ChTRPz from the citrate-rich phase to the PEG-rich phase. Temperature 293 K. ATPS compositions: PEG1450/citrate pH 5.20 TLL 22.3% (w/w); PEG3350/citrate pH 5.20 TLL 24.2% (w/w); PEG8000/citrate pH 5.20 TLL 22.6% (w/w).

Previous works have demonstrated that protein partitioning behaviour is sensitive to the surface hydrophobicity [22,10]. A high hydrophobic character of a biomolecule is a factor that favours the partition equilibrium displacement to the PEG-rich phase [23]. Since TRPz showed a S_o value nearly twofold that of ChTRPz, $K_{p_{TRPz}}$ values would be expected to be higher than the $K_{p_{ChTRPz}}$ ones. However, this prediction does not agree with our experimental observations since $K_{p_{TRPz}}$ is lower than $K_{p_{ChTRPz}}$ for most of the assayed systems. This behaviour is indicating that other strong enthalpic forces than protein hydrophobicity are operating in protein partitioning, such as cost of energy in cavity formation in the citrate-rich phase (salting-out) and cost in energy of transferring counter ion to the PEG-rich phase [17].

3.4. Selection of optimal separating conditions

The theoretical recovery (R) and purity percentage (P) of TRPz that it would be obtained in the bottom phase after one extraction step, were calculated from the measured K_p values of each protein in order to select the ATPS with the best separating capability. Several assumptions were made. The partitioned sample was considered to be formed by equal quantities of the target protein (TRPz) and its main contaminant (ChTRPz), as it occurs in the pancreatic homogenate composition. The top/bottom volume ratio was assumed to be 1 and the K_p values measured for each protein separately were considered to be invariant when the proteins are forming a mixture. The effect of PEG molecular weight, pH and tie line length on the R and P values are shown in Fig. 5. It is evident that ATPSs of high molecular weight lead to high TRPz yields (about of

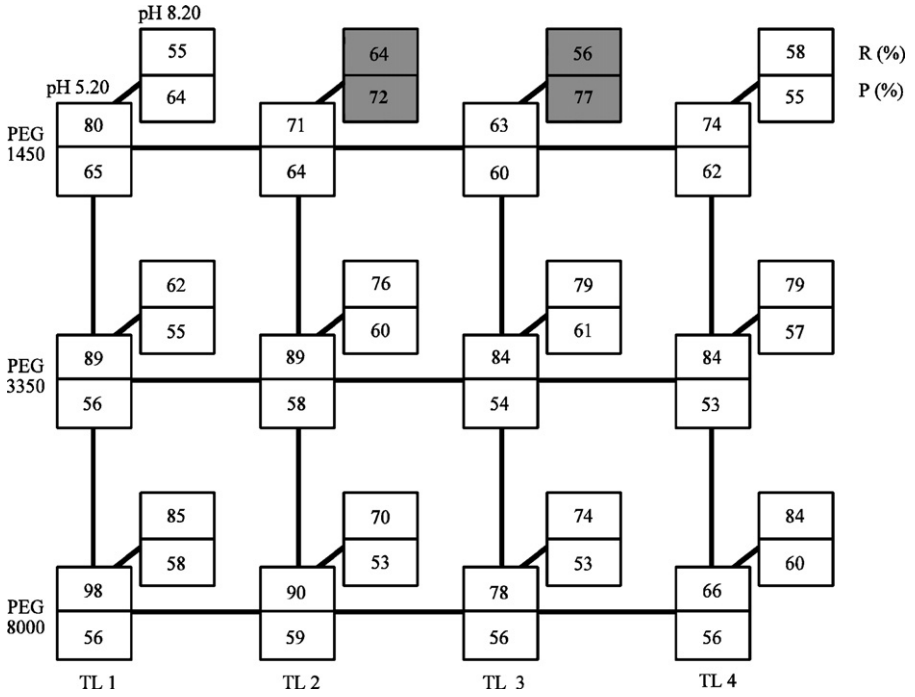

Fig. 5. The effect of PEG molecular weight, pH and tie line length on the *R* (%) and *P* (%) of TRPz in the citrate-rich phase after one extraction effect. Volume ratio equal to 1.

80–90%), which agrees with the lowest observed K_p values. However, these systems have a disadvantage, since polymers of large size are difficult to remove from the protein after partitioning. In contrast, ATPSs formed by smaller PEGs led to higher TRPz purity values. In this way, PEG1450/citrate pH 8.20 ATPSs with compositions corresponding to the tie line 2 and 3 were selected for further study since they would allow us to obtain a highly pure protein with reasonable recoveries.

3.5. Purification of TRPz from a mixture TRPz/ChTRPz

In order to experimentally verify the calculated results, a mixture of both proteins TRPz and ChTRPz was partitioned in the selected two-phase systems. Fig. 6 shows the TRPz recovery and purity measured for the assayed systems. The measured *P* and *R* were observed to differ from the previously calculated values (one extraction step and $V_T/V_B = 1$). This behaviour may be attributed to the difference between the partition coefficients of TRPz and ChTRPz separately and in an artificial mixture due to the presence of a protein–protein interaction [23]. The effects of another two variables, the top–bottom volume ratio and the number of extractive steps on the TRPz purification were assayed in order to enhance the efficiency of the systems. By increasing the top–bottom volume ratio from 1 to 4, a significant increase in the purity with loss of recovery was observed for the two assayed tie lines. A second extractive step was developed by removing the top phase and replacing it by identical volume of this phase without protein. In this case, a significant enhancement of TRPz purity was observed (89%) for the composition of tie line 2. Although both alternatives led to an improvement in the TRPz purity in the bottom phase, the latter strategy proved to be the most adequate one since it allowed us to obtain TRPz with the highest purity (89%) and similar recovery (34%).

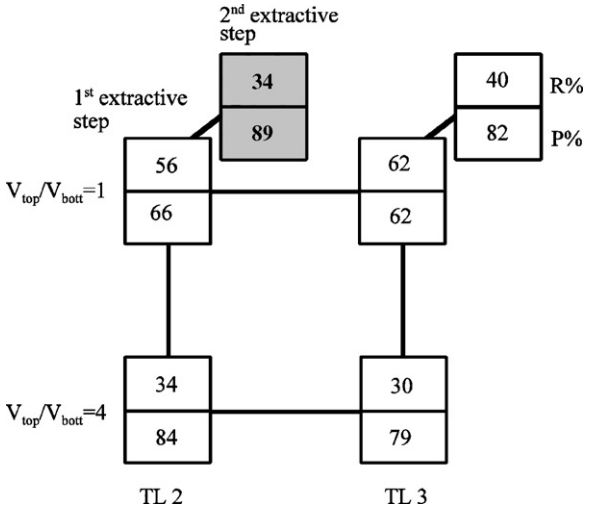

Fig. 6. Effect of number of extractive steps and volume ratio on the recovery and purity of TRPz after partitioning a mixture formed by equal quantities of TRPz and ChTRPz in the selected ATPSs with compositions of tie lines 2 and 3. Temperature 20 °C.

4. Conclusions

In this work, TRPz and ChTRPz partitioning behaviour in the assayed ATPSs showed similarities and differences. K_p of both zymogens proved to be very sensitive to pH and PEG molecular weight due to the electrical protein charge and the exclusion effect, respectively. Our thermodynamical approach showed that an entropic–enthalpic compensation pattern was associated with the TRPz and ChTRPz transfer from the bottom to the top phase, thus indicating the participation of water molecules in the partitioning mechanism.

The different partitioning behaviour of TRPz and ChTRPz leads to a practical application. ATPSs of PEG1450-pH 8.20 with compositions corresponding to the tie line 2 and 3 showed to be efficient for separating both proteins. When a mixture formed by equal quantities of TRPz and ChTRPz was partitioned in the selected systems ($V_T/V_B = 1$), good TRPz yields were obtained in the two sys-

tems (about of 60%) without significant purity values (62–66%). By increasing V_t/V_B to 4 or adding a new partitioning step, the latter variable was enhanced to 84–89% with a moderate loss of recovery (34%).

Finally, we know that the present study would be fully completed when the partitioning of the natural source of TRPz and ChTRPz, i.e. bovine pancreatic homogenate, was assayed in the selected ATPSs. Then, a further optimization of process variables will be required. Although this, the low cost of the phase-forming components, the biodegradability of citrate and the promising results with artificial mixtures allow us to consider these ATPSs as a viable and potentially useful tool for the separation of TRPz and ChTRPz.

Acknowledgements

This work was supported by a grant from FoNCyT no. 06-12476/02 and PIP 5053 CONICET. We thank Nuevo Banco de Santa Fe Foundation for supporting Luciana Pellegrini Malpiedi's grant. We also thank María Robson and Marcela Culasso for the language correction of this manuscript.

References

[1] B.Y. Zaslavsky, Aqueous Two-Phase Partitioning. Physical Chemistry and Bioanalytical Applications, Marcel Dekker Inc., New York, 1994.
[2] P.A. Albertsson, Partition of Cell Particles and Macromolecules, 2nd ed., John Wiley and Sons, New York, 1971.
[3] R. Hatti-Kaul, Methods in Biotechnology. Aqueous Two-Phase Systems. Methods and Protocols, Humana Press, New Jersey, 2000.
[4] J.C. Marcos, L.P. Fonseca, M.T. Ramalho, J.M.S. Cabral, J. Chromatogr. B 734 (1999) 15.
[5] J. Alves, L. Chumpitaz, L. da Silva, T. Franco, A. Meirelles, J. Chromatogr. B 743 (2000) 235.
[6] S. Woodard, J. Mayor, M. Bailey, D. Barker, R. Love, J. Lane, D. Delaney, J. McComas-Wagner, H. Mallubhotla, E. Hood, L. Dangott, S. Tichy, J.A. Howard, Biotechnol. Appl. Biochem. 38 (2003) 123.
[7] K. Johnson, A. Clark, S. Marshall, Comp. Biochem. Physiol. B 131 (2002) 423.
[8] N. Sreerama, R.W. Woody, Anal. Biochem. 287 (2000) 252.
[9] C.V. Haskard, E.C. Li-Chan, J. Agric. Food Chem. 46 (1998) 2671.
[10] G. Tubio, B. Nerli, G. Picó, J. Chromatogr. B 799 (2004) 293.
[11] G. Tubío, L. Pellegrini, G. Picó, B. Nerli, J. Chem. Eng. Data 51 (2006) 209.
[12] J. Kay, B. Kassell, J. Biol. Chem. 246 (1971) 6661.
[13] A. Gildberg, K. Overbo, Comp. Biochem. Physiol. B 97 (1990) 775.
[14] B. Lebreton, A. Lyddiatt, J. Chromatogr. B 743 (2000) 263.
[15] N. Skeerama, R. Woody, Protein Sci. 12 (2003) 384.
[16] D. Forciniti, C.K. Hall, M.R. Kula, Biotech. Bioeng. 38 (1991) 986.
[17] H.O. Johansson, G. Karlstrom, F. Tjerneld, C. Haynes, J. Chromatogr. B 711 (1998) 3.
[18] K.P. Ananthapadmanabhan, E. Goddard, Langmuir 3 (1987) 25.
[19] A. Diamond, J. Hsu, AIChE J. 36 (1990) 1017.
[20] B. Farruggia, B. Nerli, H. Di Nuci, R. Rigatusso, G. Picó, Int. J. Biol. Macromol. 26 (1999) 23.
[21] R. Lumry, S. Rajender, Biopolymers 9 (1970) 1125.
[22] N. Gulyaeva, A. Zaslavsky, P. Lechner, A. Chait, B. Zaslavsky, J. Chromatogr. B 743 (2000) 187.
[23] T. Franco, A. Andrews, A. Asenjo, Biotechnol. Bioeng. 49 (1996) 309.